

# Instabilities in dark coupled models and constraints from cosmological data

Laura Lopez Honorez\* and Olga Mena†

\**Departamento de Física Teórica & Instituto de Física Teórica,  
Universidad Autónoma de Madrid, 28049 Cantoblanco, Madrid, Spain and  
Service de Physique Théorique, Université Libre de Bruxelles, 1050 Brussels, Belgium*  
†*Instituto de Física Corpuscular, IFIC, CSIC and Universidad de Valencia, Spain*

**Abstract.** Coupled dark matter-dark energy systems can suffer from non-adiabatic instabilities at early times and large scales. In these proceedings, we consider two parameterizations of the dark sector interaction. In the first one the energy-momentum transfer 4-vector is parallel to the dark matter 4-velocity and in the second one to the dark energy 4-velocity. In these cases, coupled models which suffer from non-adiabatic instabilities can be identified as a function of a generic coupling  $Q$  and of the dark energy equation of state  $w$ . In our analysis, we do not refer to any particular cosmic field. We confront then a viable class of models in which the interaction is directly proportional to the dark energy density and to the Hubble rate parameter to recent cosmological data. In that framework, we show that correlations between the dark coupling and several cosmological parameters allow for a larger neutrino mass than in uncoupled models.

**Keywords:** dark energy, dark matter, perturbation theory, cosmology of theories beyond the SM  
**PACS:** 98.80.Cq, 98.80.Es

## INTRODUCTION

Interactions between dark matter and dark energy are still allowed by observational data today. At the level of the background evolution equations, one can generally introduce a coupling between these two sectors as follows:

$$\dot{\rho}_{dm} + 3\mathcal{H}\rho_{dm} = Q, \quad (1)$$

$$\dot{\rho}_{de} + 3\mathcal{H}\rho_{de}(1+w) = -Q. \quad (2)$$

$\rho_{dm}(\rho_{de})$  denotes the dark matter (dark energy) energy density, the dot indicates derivative with respect to conformal time  $d\tau = dt/a$ ,  $\mathcal{H} = \dot{a}/a$  and  $w = P_{de}/\rho_{de}$  is the dark-energy equation of state ( $P$  denotes the pressure). We work with the Friedman-Robertson-Walker (FRW) metric, assuming a flat universe and pressureless dark matter  $w_{dm} = P_{dm}/\rho_{dm} = 0$ .

$Q$  encodes the dark coupling and drives the energy exchange between dark matter and dark energy. For *e.g.*  $Q < 0$  the energy flows from dark matter to dark energy. It also changes the dark matter and dark energy redshift dependence acting as an extra contribution to their effective equation of state. For *e.g.*  $Q < 0$ , dark matter redshifts faster, as a consequence, there is more dark matter in the past compared to uncoupled scenarios assuming that the dark matter density today is the same in the two models (see also the discussion in Ref. [1]). This general feature of coupled models is sketched in Fig. 1 (for a particular form of  $Q$ , see also Fig. 2).

Also notice that a universe in accelerated expansion today requires  $w < -1/3$  even in the presence of a dark coupling. Indeed, the deceleration parameter satisfies

$$q = -\frac{\mathcal{H}}{\mathcal{H}^2} = \frac{1}{2}(1 + 3w\Omega_{de}), \quad (3)$$

either with or without dark coupling. The curvature contribution has been neglected in this equation.

In order to deduce the evolution of density and velocity perturbations in coupled models, we need an expression of the energy transfer in terms of the stress-energy tensor:

$$\nabla_{\mu}T^{\mu}_{(dm)v} = Q_v \quad \text{and} \quad \nabla_{\mu}T^{\mu}_{(de)v} = -Q_v. \quad (4)$$

The 4-vector  $Q_v$  governs the energy-momentum transfer between the dark components and  $T^{\mu}_{(dm)v}$  and  $T^{\mu}_{(de)v}$  are the energy-momentum tensors for the dark matter and dark energy, respectively. Equation (4) guaranties the conservation

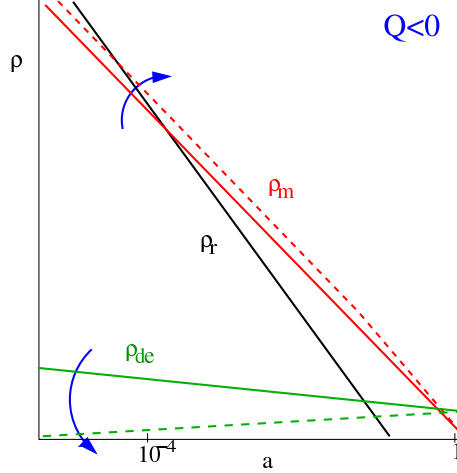


**FIGURE 1.** This figure illustrates roughly the effect of a negative dark coupling term  $Q$  on dark matter and dark energy evolution.  $a$  is the scale factor,  $\rho_i$  with  $i = m, r, de$  corresponds to matter (dark matter plus baryon), radiation and dark energy densities respectively. Solid curve account for an uncoupled model with constant dark energy equation of state  $w > -1$  and dotted curve for coupled models with  $Q < 0$  with  $w > -1$ .

of the total energy-momentum tensor. In the following we consider two scenarios which reproduce at the background level Eqs. (1) and (2):

1.  $Q_V$  is parallel to the dark matter four velocity  $u_V^{(dm)}$ :

$$Q_V = Q u_V^{(dm)} / a. \quad (5)$$

This choice of parameterization, which was first proposed in Ref. [2], avoids momentum transfer in the rest frame of dark matter (*i.e.*  $v_{(dm)}^i = 0$ ),

2.  $Q_V$  is parallel to the dark energy four velocity  $u_V^{(de)}$ :

$$Q_V = Q u_V^{(de)} / a. \quad (6)$$

In this case the dark matter velocity (Euler) equation is modified by the coupling and the weak equivalence principle is violated (see *e.g.* Ref [3] for a recent discussion). Notice that one example for this interaction is  $Q_V = \beta \rho_{dm} \nabla_V \phi$  [4, 5], where  $\phi$  would be a coupled dark energy scalar field and  $u_V^{(de)} \propto \nabla_V \phi$ .

It was first pointed out in Ref. [2] that the dark coupling terms which appears in the non-adiabatic dark energy pressure perturbations are a source for early time instabilities at large scales for coupled models satisfying Eqs. (4) and (5). Their analysis was however restricted to  $Q > 0$  proportional to the dark matter density, in which case the coupled model is particularly unstable for a constant dark energy equation of state. Non-adiabatic instabilities were subsequently analyzed by several authors, and it was proved that the stability depends on the type of dark coupling  $Q$ , on the dark energy equation of state  $w$  and on the  $Q_V$  4-velocity dependence, see Ref. [6, 7, 8, 9] (for similar instabilities pointed out in coupled quintessence models, see Ref. [10, 11]).

Among these references, we proposed in Ref. [8], a criteria associated to the dubbed *doom factor* to identify the stability region of coupled models with a constant dark energy equation of state  $w$  satisfying Eqs. (4) and (5). The doom factor is a function of the model parameters such as  $Q$  and  $w$ , but it is defined independently of the explicit form of the coupling  $Q$ . We review this result in the next section and extend it to models satisfying Eqs. (4) and (6).

Based on this analysis, we study the compatibility of a successful class of models, in which  $Q$  is proportional to the dark energy density, with a fixed dataset including WMAP 5 year [12, 13], HST [14], SN [15],  $H(z)$  [16] and LSS [17] data. This work was done using the publicly available CAMB code [18] and `cosmomc` package [19]. The latter were modified in order to include the interaction between the dark matter and dark energy components and the modified dark matter velocity equation in the case of coupled models satisfying Eq. (6) (see Eq. (18)). Present data will be shown to allow for a sizeable interaction strength and to imply weaker cosmological limits on neutrino masses with respect to non-interacting scenarios.

## ORIGIN OF NON-ADIABATIC INSTABILITIES

Non-adiabatic instabilities arise at linear order in perturbations and appear to be driven by the dark coupling term present in the non-adiabatic dark energy pressure perturbation [2]. Using the definitions of gauge invariant density perturbation and entropy perturbation (see *e.g.* Ref. [20]), one can work out a general expression which relates the dark energy pressure perturbation  $\delta P_{de}$  in its rest frame to the one in any other frame. The former is characterized by  $\hat{c}_{sde}^2 = [\delta P_{de}/\delta \rho_{de}]_{\text{rf}}$ , the propagation speed of pressure fluctuations in the rest frame of dark energy which has to be distinguished from  $c_{ade}^2 = \dot{P}_{de}/\dot{\rho}_{de}$ , the so called ‘‘adiabatic sound speed’’. In the synchronous or the Newtonian gauge, one obtains:

$$\delta P_{de} = \hat{c}_{sde}^2 \delta \rho_{de} + (\hat{c}_{sde}^2 - c_{ade}^2) \dot{\rho}_{de} \frac{\theta_{de}}{k^2}, \quad (7)$$

where  $\delta \rho_{de}$  denotes the dark energy density perturbation and  $\theta_{de} \equiv \partial_i v_{(de)}^i$  is the divergence of the dark energy proper velocity,  $v_{(de)}^i$ . Using equation (2), we see that the dark coupling resulting from the  $\dot{\rho}_{de}$  term directly affects the  $\delta P_{de}$ . In Eq. (8), we rewrite Eq. (7) in term of the dubbed doom factor  $\mathbf{d} \propto Q$  which is a useful tool to spot the combined role of  $Q$  and  $w$  in driving the non-adiabatic instabilities. In the following we illustrate this feature in the framework of coupled models satisfying Eqs. (5) and (6).

Notice that non-adiabatic instabilities differ from the adiabatic ones. The latter appear at relatively small scales and late times. In the adiabatic regime, the effective sound speed of the fluid tends towards the adiabatic one which turns out to be negative [21, 22, 23]. As a consequence, pressure no longer counteracts the effect of gravity and instabilities can breakout.

In the following, we work with constant equation of state  $w$  in which case ( $c_{ade}^2 = w$ ) and we assume that our universe is in accelerating expansion today, which implies that  $w < -1/3$ . Moreover, we restrict our analysis to the case  $\hat{c}_{sde}^2 > 0$  and  $\hat{c}_{sde}^2 = 1$  will be assumed for numerical computation.

## GROWTH EQUATION AT LARGE SCALES AND THE DOOM FACTOR

A cartoon equation of the growth equation governing the evolution of energy density linear perturbation for any species  $i, j$  is given by:

$$\delta_i'' = \underbrace{A_i \frac{\delta_i}{a^2}}_{\text{Exponential Growth or Oscillations}} + \underbrace{B_i \frac{\delta_i'}{a}}_{\text{(Anti)Damping}} + \underbrace{\mathcal{F}(\rho_j, \delta_j, \delta_j'; j \neq i)}_{\text{leads when A,B negligible}}$$

where  $\delta_i = \delta \rho_i / \rho_i$  and the prime denotes a derivative with respect to the scale factor  $' = \partial / \partial a$ . The evolution of a perturbation depends on the relative weight of the three terms present in this equation *and* on their signs:

1. For positive  $A$ , the  $A$  and  $B$  terms taken by themselves would induce a rapid growth of the perturbation, which may be damped or antidamped (reinforced) depending on whether  $B$  is negative or positive, respectively. In particular, for  $A$  and  $B$  both positive, the solution may enter in an exponentially growing, unstable, regime.
2. For negative  $A$ , in contrast, the  $A$  and  $B$  terms taken alone describe a harmonic oscillator, with oscillations damped (antidamped) if  $B$  is negative (positive). In the  $A, B < 0$  regime, the third term may play in fact the leading role.

In the standard uncoupled scenario, the dark matter perturbations behave as in case 1 above (with  $A > 0$  and  $B < 0$ ), while the dark energy ones provide an example of behavior as in case 2.

For coupled models, we concentrate on the case in which the dark-coupling terms dominate over the usual one, in order to put forward the presence of non adiabatic instabilities (see Ref.[8] for more details). For this purpose, let us rewrite Eq. (7) as:

$$\frac{\delta P_{de}}{\delta \rho_{de}} = \hat{c}_{sde}^2 + 3(\hat{c}_{sde}^2 - c_{ade}^2)(1+w)(1+\mathbf{d}) \frac{\mathcal{H} \theta_{de}}{k^2 \delta_{de}}, \quad (8)$$

where  $\mathbf{d}$  refers to the doom factor which we have defined as:

$$\mathbf{d} \equiv \frac{Q}{3\mathcal{H}\rho_{de}(1+w)}. \quad (9)$$

The *strong coupling regime* can be characterized by  $|\mathbf{d}| > 1$ , which also guarantees that the interaction among the two dark sectors drives the non-adiabatic contribution to the dark energy pressure perturbation.

In Ref. [8], the strong coupling regime analysis was restricted to coupled models satisfying Eqs. (4) and (5). It is however rather straightforward to generalize this result to models satisfying Eq. (6) (see also the appendix). At large scales-early times ( $\mathcal{H}/k \gg 1$ ), the leading contributions in  $Q$ , or equivalently in  $\mathbf{d}$ , to the second order differential equation for  $\delta_{de}$  reads:

$$\delta_{de}'' \simeq 3\mathbf{d}(\hat{c}_{sde}^2 + b) \left( \frac{\delta_{de}'}{a} + 3b \frac{\delta_{de}}{a^2} \frac{(\hat{c}_{sde}^2 - w)}{\hat{c}_{sde}^2 + b} + \frac{3(1+w)}{a^2} \delta[\mathbf{d}] \right) + \dots \quad (10)$$

where we use the  $b$  notation introduced in Ref. [6],  $b = 1$  stands for models with  $Q_v \propto u_v^{(dm)}$  (5) and  $b = 0$  for models with  $Q_v \propto u_v^{(de)}$  (6). The sign of the coefficient  $B_e$  of  $\delta_{de}'$  in this expression is crucial for the analysis of instabilities. Assuming  $\hat{c}_{sde}^2 > 0$ , it reduces to the sign of the doom factor  $\mathbf{d}$ . As previously argued, a positive  $\mathbf{d}$  can trigger large scale instabilities. Similar second order differential equations for  $\delta_{de}$  were obtained in Refs. [6, 7] for particular expressions of the dark coupling  $Q$  and an analytical form of their solutions were derived in order to determine when  $\delta_{de}$  blows up. In particular, the results of Ref. [7] confirm those of Ref. [2] for positive  $Q \propto \rho_{dm}$  and  $1+w > 0$ . In addition, our Eq. (10) reproduces as well the dark coupling leading contributions of Ref. [6], which studied  $Q \propto \rho_{de}$  coupled models, in particular, they carried out the first stability analysis in the framework of  $Q_v \propto \rho_{de} u_v^{(de)}$ .

### VIABLE MODELS: $Q \propto \rho_{de}$

Using the tools that we have developed in the previous section, we can now easily verify that for

$$Q = \xi \mathcal{H} \rho_{de}, \quad (11)$$

we have rather simple and viable models for specific combination of  $1+w$  and of the dimensionless constant coupling  $\xi$ . Indeed in these models the doom factor of Eq. (9) is given by:

$$\mathbf{d} = \frac{\xi}{3(1+w)}. \quad (12)$$

When  $\mathbf{d} < 0$ , that is, for  $\xi < 0$  and  $1+w > 0$  (or  $\xi > 0$  and  $1+w < 0$ ), no instabilities are expected and we can safely fit the coupled models to cosmological data. Notice that this result is in agreement with those of Refs. [7, 6] which restricted though their stability analysis to the  $\xi > 0$  case.

For the sake of completeness we first give the expressions of the background dark fluids energy densities and first order perturbation evolution equations which were introduced in the CAMB code [18]. As previously mentioned, we work in the synchronous gauge.

### Background

The solutions to Eqs. (1) and (2) using Eq (11) are:

$$\rho_{dm} = \rho_{dm}^{(0)} a^{-3} + \rho_{de}^{(0)} \frac{\xi}{3w + \xi} (1 - a^{-3w - \xi}) a^{-3}, \quad (13)$$

$$\rho_{de} = \rho_{de}^{(0)} a^{-3(1+w) + \xi}. \quad (14)$$

The dark energy density is thus always positive, all along the cosmic evolution and since its initial moment. To ensure that the same happens with the dark matter density, all values of  $w < 0$  are acceptable for  $\xi < 0$ , while for positive  $\xi$  it is required that

$$\xi \lesssim -w.$$

In Fig. 2, we see that negative (positive) couplings lead to more (less) dark matter in the past than in the uncoupled case. In the following we focus on negative couplings in order to avoid non-adiabatic instabilities.

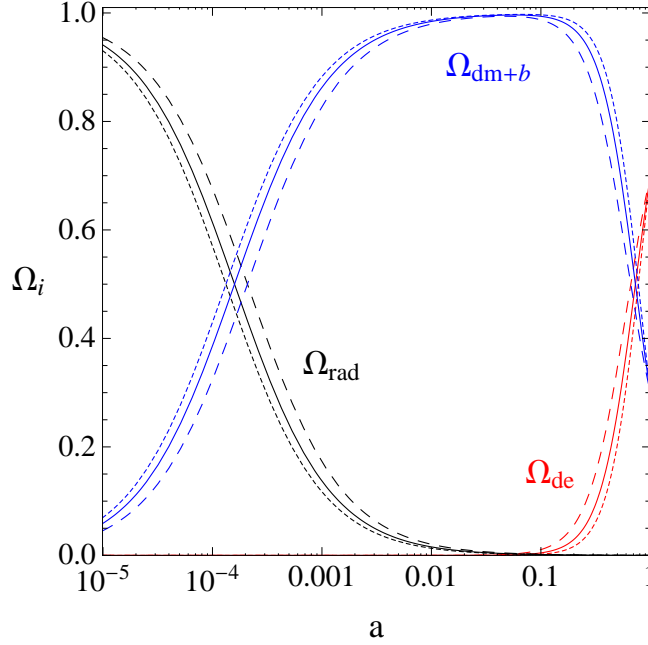


**FIGURE 2.** Scenario with  $Q \propto \rho_{de}$ . Relative energy densities of dark matter plus baryons  $\Omega_{dm+b}$  (blue), radiation  $\Omega_{rad}$  (black) and dark energy  $\Omega_{de}$  (red), as a function of the scale factor  $a$ , for  $w=-0.9$ . Three values of the coupling are illustrated:  $\xi = 0$  (solid curve), 0.25 (long dashed curve) and  $-0.25$  (short dashed curve).

## Linear perturbation theory

In the synchronous comoving gauge, metric scalar perturbations are described by the two usual fields [24]  $h(x, \tau)$  and  $\eta(x, \tau)$ . Defining  $\delta \equiv \delta\rho/\rho$  for the fluid density perturbations,  $\theta \equiv \partial_i v^i$  for the divergence of the fluid proper velocity  $v^i$  and using Eq. (4), it results, at first order in perturbation theory:

$$\dot{\delta}_{dm} = -(\theta_{dm} + \frac{1}{2}\dot{h}) + \xi \mathcal{H} \frac{\rho_{de}}{\rho_{dm}} (\delta_{de} - \delta_{dm}) \quad (15)$$

$$\dot{\theta}_{dm} = -\mathcal{H} \theta_{dm} + \xi \mathcal{H} (1-b) \frac{\rho_{de}}{\rho_{dm}} (\theta_{de} - \theta_{dm}). \quad (16)$$

$$\dot{\delta}_{de} = -(1+w)(\theta_{de} + \frac{1}{2}\dot{h}) - 3\mathcal{H} (\hat{c}_{sde}^2 - w) \left[ \delta_{de} + \mathcal{H} (3(1+w) + \xi) \frac{\theta_{de}}{k^2} \right], \quad (17)$$

$$\dot{\theta}_{de} = -\mathcal{H} \left( 1 - 3\hat{c}_{sde}^2 - \frac{\hat{c}_{sde}^2 + b}{1+w} \xi \right) \theta_{de} + \frac{k^2}{1+w} \hat{c}_{sde}^2 \delta_{de} - b \xi \mathcal{H} \frac{\theta_{dm}}{1+w}, \quad (18)$$

where  $b = 1$  stands for models with  $Q_v \propto u_v^{(dm)}$  (5) and  $b = 0$  for models with  $Q_v \propto u_v^{(de)}$  (6). We have assumed that  $\mathcal{H}$  is the global expansion rate and that it does not contribute to  $Q$  perturbation.

Notice that the continuity equation for dark matter (15) always includes an extra term compared to uncoupled models which depends on the dark interaction  $Q$  of Eq. (11). Focusing on viable models, it can be shown<sup>1</sup> that the dark matter growth equation at small scales is mainly modified in two ways: (i) the background evolution (in particular,  $\rho_{dm}$

<sup>1</sup> See [3] for similar coupled models. The details of the growth at small scales associated to the models studied here will be presented elsewhere.

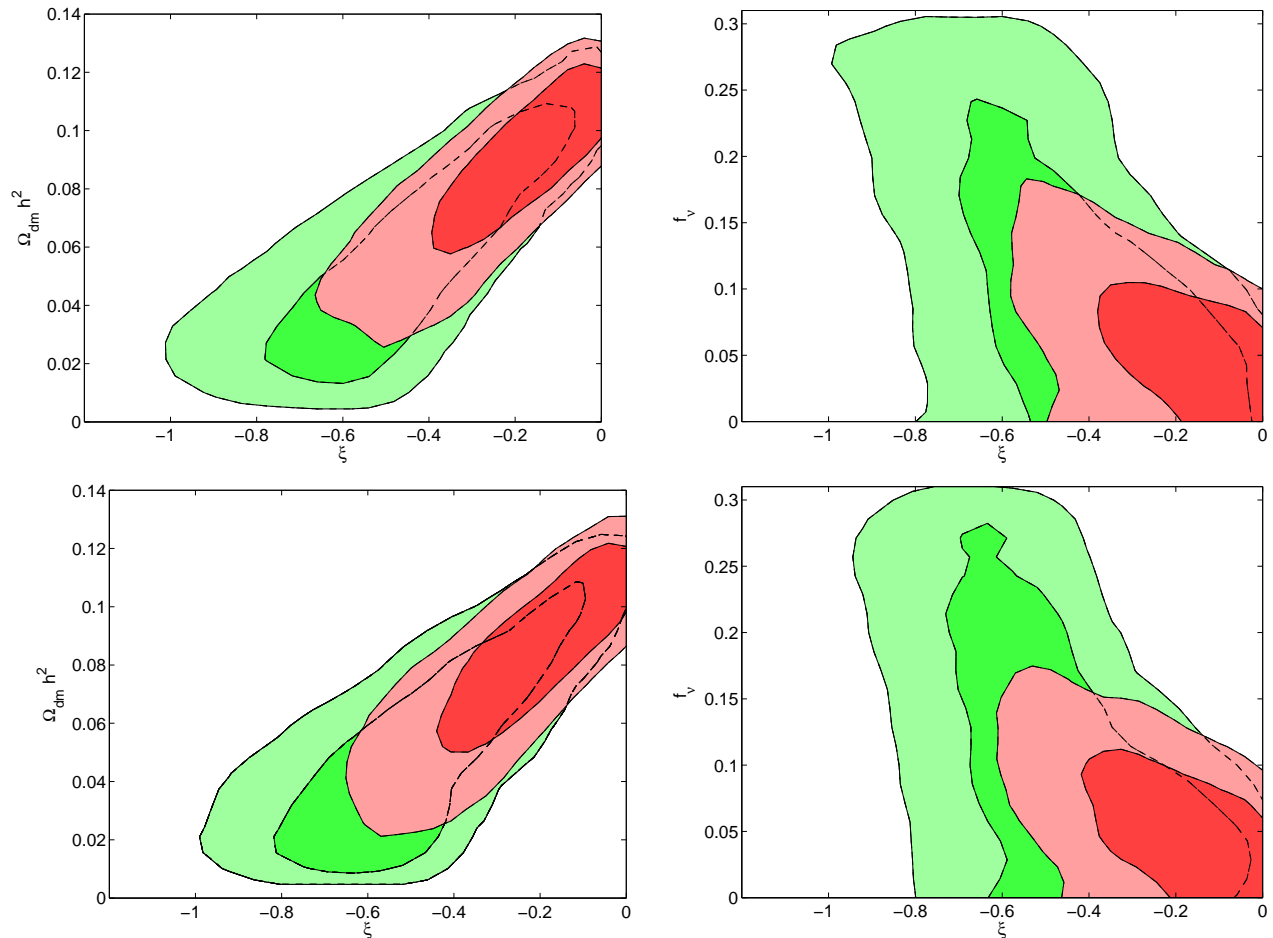


**FIGURE 3.** Scenario with  $Q \propto \rho_{de}$ . The two upper panels correspond to models with  $Q_v \propto u_v^{(dm)}$ , the two lower panels to models with  $Q_v \propto u_v^{(de)}$ . Left (right) panel:  $1\sigma$  and  $2\sigma$  marginalized contours in the  $\xi$ - $\Omega_{dm}h^2$  ( $\xi$ - $f_v$ ) plane. The largest, green contours show the current constraints from WMAP (5 year data), HST, SN and  $H(z)$  data. The smallest, red contours show the current constraints from WMAP (5 year data), HST, SN,  $H(z)$  and LSS data.

and  $\mathcal{H}$  evolution) is different, (ii) the Hubble friction term and the source term get extra contributions from  $Q$ . For negative couplings, these two modifications lead to an enhancement of the dark matter growth compared to uncoupled models (see also Ref. [1] for similar models). The closer  $\xi$  gets to -1, the larger is the growth. This particular feature can be constrained by cosmological data, in particular in the next section we will see that large scale structure data provide the strongest limits on the interaction  $Q$ .

Also notice that the Euler equation for dark matter (16) is only modified in the  $Q_v \propto u_v^{(de)}$  (6) case, leading a violation of the weak equivalence principle. Constraints resulting from the difference between dark matter and baryon velocities could provide additional restrictions on the allowed values of the dark coupling, to be added to the ones presented in the following section. For the sake of comparison with the already studied  $Q_v \propto u_v^{(dm)}$  (5) model we present below the likelihood plots for the two coupled models (5) and (6).

### COSMOLOGICAL CONSTRAINTS FROM DATA FOR $Q = \xi \mathcal{H} \rho_{de}$

In Ref. [8], we explore the constraints on the dark energy-dark matter coupling  $\xi$  using the publicly available package `cosmomc` [19]. The latter is modified in order to include the coupling among the dark matter and dark energy components. More details on the cosmological model and on the priors adopted can be found in Ref. [8]. The datasets

in the analysis are:

1. WMAP 5-year data [12, 13]
2. Prior on the Hubble parameter of  $72 \pm 8$  km/s/Mpc from the Hubble key project (HST) [14]
3. Super Novae Ia (SN Ia) data [15]
4.  $H(z)$  data at  $0 < z < 1.8$  from galaxy ages [16]
5. Large scale structure data (LSS data) from the Sloan Digital Sky Survey [17]

The data analysis is carried out into two runs, the first run includes the datasets from 1 to 4 while in the second run the fifth dataset is added. We restrict ourselves to  $w > -1$  and  $\xi < 0$ , a parameter region which ensures a negative doom factor, see Eq. (12), and thus spans an instability-free region of scenarios to explore.

Figure 3 (left panel) illustrates the 1 and 2 $\sigma$  marginalized contours in the  $\xi$ - $\Omega_{dm}h^2$  plane, where  $\Omega_{dm}$  is today's ratio between dark matter energy density and critical energy density. The results from the two runs described above are shown. Notice that a huge degeneracy is present, being  $\xi$  and  $\Omega_{dm}h^2$  positively correlated. The shape of the contours can be easily understood following our discussion in the previous sections. In a universe with a negative dark coupling  $\xi$ , there is an enhancement of the growth of structure relative to the non interacting case. The amount of *intrinsic* dark matter (which is directly proportional to  $\Omega_{dm}h^2$ ) needed to reproduce the LSS data should decrease as the dark coupling becomes more and more negative. We also see that the addition of LSS data in the second run (red contours in Figs. 3 and 4) gives the most stringent constraint on  $\xi$ .

The right panel of Fig. 3 shows the correlation among the fraction of matter energy-density in the form of massive neutrinos  $f_\nu$  and the dark coupling  $\xi$ . The relation between the neutrino fraction used here  $f_\nu$  and the neutrino mass for  $N_\nu$  degenerate neutrinos reads

$$f_\nu = \frac{\Omega_\nu h^2}{\Omega_{dm} h^2} = \frac{\sum m_\nu}{93.2 \text{eV}} \cdot \frac{1}{\Omega_{dm} h^2} = \frac{N_\nu m_\nu}{93.2 \text{eV}} \cdot \frac{1}{\Omega_{dm} h^2}. \quad (19)$$

Neutrinos can indeed play a relevant role in large scale structure formation and leave key signatures in several cosmological datasets. Degeneracies between dark energy sector parameters and  $\sum m_\nu$  are rather well known, see Ref. [25, 26, 27]. Non-relativistic neutrinos in the recent Universe suppress the growth of matter density fluctuations and galaxy clustering. This effect can be compensated by the existence of a coupling between the dark sectors, due to the fact that in the coupled model negative couplings enhance the growth of matter density perturbations.

Notice that the constraints on the  $Q_\nu \propto u_\nu^{(dm)}$  (5) and  $Q_\nu \propto u_\nu^{(de)}$  (6) models are rather equivalent, due to the fact that the background evolution history (see Eqs. (13) and (14)) is the same, and the evolution of perturbations (15) - (18) is also very similar for these two models.

## CONCLUSIONS

In these proceedings, we discuss the origin of non-adiabatic instabilities in coupled models satisfying

$\nabla_\mu T_{dm}^\mu = Q u_\nu^{dm(de)}/a$  and  $\nabla_\mu T_{de}^\mu = Q u_\nu^{dm(de)}/a$ . We show that the sign of the doom factor

$$\mathbf{d} \equiv \frac{Q}{3\mathcal{H}\rho_{de}(1+w)} \quad (20)$$

reveals the presence of instabilities. In particular, when  $\mathbf{d}$  is positive and sizeable,  $\mathbf{d} > 1$ , the dark-coupling dependent terms may dominate the evolution of the dark energy perturbation, and drive an unstable growth regime. Notice that  $\mathbf{d}$  has been defined for a constant dark energy equation of state  $w$  (see *e.g.* Ref. [9, 28] for  $w = w(a)$ ).

We have studied the constraints from current cosmological data on the dimensionless coupling  $\xi$  in a class of viable models in which  $Q = \xi \mathcal{H} \rho_{de}$ , independently of the dark interaction term 4-velocity dependence. The analyses presented here were carried out in the  $\xi < 0$  and positive  $(1+w)$  region of the parameter space, which offers the best agreement with data on large scale structure formation. From the results of our fits we find that both  $w$  and  $\xi$  are not very constrained from data: it can be noticed from Fig. 4 that substantial values for both parameters, near -0.5, are easily allowed. Furthermore,  $\xi$  turns out to be positively correlated with  $\Omega_{dm}h^2$  and a larger neutrino fraction  $f_\nu$  than in uncoupled models is allowed for negative values of the coupling  $\xi$ .

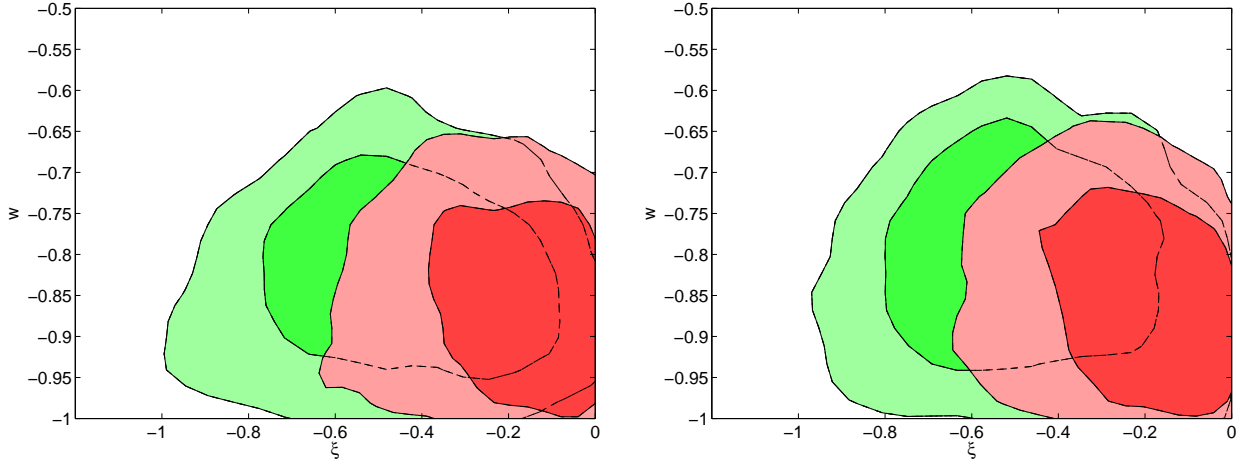


**FIGURE 4.** Scenario with  $Q \propto \rho_{de}$ . Left (right) panel:  $1\sigma$  and  $2\sigma$  marginalized contours in the  $\xi$ - $w$  plane for  $Q_V \propto u_V^{(dm)}$  ( $Q_V \propto u_V^{(de)}$ ). The largest, green contours show the current constraints from WMAP (5 year data), HST, SN and  $H(z)$  data. The smallest, red contours show the current constraints from WMAP (5 year data), HST, SN,  $H(z)$  and LSS data.

## ACKNOWLEDGMENTS

The work reported associated to the  $Q_V \propto u_V^{(dm)}$  models has been done in collaboration with B. Gavela, D. Hernandez, O. Mena and S. Rigolin, see Ref. [8]. L. L. H thanks the organizers of the Invisible Universe conference (Paris) for giving her the opportunity to give a talk on “dark couplings” and the I.F.I.C. group (Valencia), where part of the  $Q_V \propto u_V^{(de)}$  work was carried out, for its hospitality. We also acknowledge R. Jiménez B. Reid and L. Verde for useful comments and discussions. L. L. H was partially supported by CICYT through the project FPA2006-05423, by CAM through the project HEPHACOS, P-ESP-00346, by the PAU (Physics of the accelerating universe) Consolider Ingenio 2010, by the F.N.R.S. and the I.I.S.N.. O. M. work is supported by a Ramón y Cajal contract from MEC, Spain

## APPENDIX: GROWTH OF PERTURBATIONS IN STRONGLY COUPLED SCENARIOS

The strong coupling regime can be characterized by

$$\left| \frac{Q}{\mathcal{H}\rho_{de}} \right| \gg |3(1+w)|, \quad (21)$$

$$\left| \frac{Q}{\mathcal{H}\rho_{de}} \frac{\hat{c}_{sde}^2 + 1}{1+w} \right| \gg |1 - 3\hat{c}_{sde}^2|, \quad (22)$$

which ensure that the dark-coupling terms dominate the evolution of both  $\delta_{de}$  and  $\theta_{de}$ . With  $c_{sde}^2 > 0$ , Eq. (21) alone is enough to define the regime.

For coupled models satisfying Eqs. (4), (5) and (6), the resulting growth equation for dark energy perturbations at large scales ( $\mathcal{H}/k \gg 1$ ) can be approximated by

$$\begin{aligned} \delta_{de}'' \simeq & \frac{\delta_{de}'}{a} \left( \frac{Q}{\mathcal{H}\rho_{de}} \frac{\hat{c}_{sde}^2 + b}{1+w} + a(\ln[Q/\rho_{de}])' \right) \\ & + 3 \frac{\delta_{de}}{a^2} (\hat{c}_{sde}^2 - w) \left( \frac{Q}{\mathcal{H}\rho_{de}} \frac{b}{1+w} + a(\ln[Q/\rho_{de}])' \right) \\ & + \frac{1}{a^2 \mathcal{H}} \delta[Q/\rho_{de}] \left( \frac{\hat{c}_{sde}^2 + b}{1+w} \frac{Q}{\mathcal{H}\rho_{de}} + a(\ln[Q/\rho_{de}])' - \frac{1}{2} - \frac{3}{2} w \Omega_{de} \right) \\ & - \frac{1}{a \mathcal{H}} (\delta[Q/\rho_{de}])' - (1+w) \frac{\dot{h}}{2}. \end{aligned} \quad (23)$$



where  $b = 1$  for models with  $Q_V \propto u_V^{(dm)}$  (5) and  $b = 0$  for models with  $Q_V \propto u_V^{(de)}$  (6).

## REFERENCES

1. G. Caldera-Cabral, R. Maartens, and B. M. Schaefer, *JCAP* **0907**, 027 (2009), 0905.0492.
2. J. Valiviita, E. Majerotto, and R. Maartens, *JCAP* **0807**, 020 (2008), 0804.0232.
3. K. Koyama, R. Maartens, and Y.-S. Song (2009), 0907.2126.
4. C. Wetterich, *Astron. Astrophys.* **301**, 321–328 (1995), hep-th/9408025.
5. L. Amendola, *Phys. Rev.* **D60**, 043501 (1999), astro-ph/9904120.
6. B. M. Jackson, A. Taylor, and A. Berera, *Phys. Rev.* **D79**, 043526 (2009), 0901.3272.
7. J.-H. He, B. Wang, and E. Abdalla, *Phys. Lett.* **B671**, 139–145 (2009), 0807.3471.
8. M. B. Gavela, D. Hernandez, L. L. Honorez, O. Mena, and S. Rigolin, *JCAP* **0907**, 034 (2009), 0901.1611.
9. E. Majerotto, J. Valiviita, and R. Maartens (2009), 0907.4981.
10. P. S. Corasaniti, *Phys. Rev.* **D78**, 083538 (2008), 0808.1646.
11. S. Chongchitnan, *Phys. Rev.* **D79**, 043522 (2009), 0810.5411.
12. J. Dunkley, et al., *Astrophys. J. Suppl.* **180**, 306–329 (2009), 0803.0586.
13. E. Komatsu, et al., *Astrophys. J. Suppl.* **180**, 330–376 (2009), 0803.0547.
14. W. L. Freedman, et al., *Astrophys. J.* **553**, 47–72 (2001), astro-ph/0012376.
15. M. Kowalski, et al., *Astrophys. J.* **686**, 749–778 (2008), 0804.4142.
16. J. Simon, L. Verde, and R. Jimenez, *Phys. Rev.* **D71**, 123001 (2005), astro-ph/0412269.
17. M. Tegmark, et al., *Phys. Rev.* **D74**, 123507 (2006), astro-ph/0608632.
18. A. Lewis, A. Challinor, and A. Lasenby, *Astrophys. J.* **538**, 473–476 (2000), astro-ph/9911177.
19. A. Lewis, and S. Bridle, *Phys. Rev.* **D66**, 103511 (2002), astro-ph/0205436.
20. H. Kodama, and M. Sasaki, *Prog. Theor. Phys. Suppl.* **78**, 1–166 (1984).
21. N. Afshordi, M. Zaldarriaga, and K. Kohri, *Phys. Rev.* **D72**, 065024 (2005), astro-ph/0506663.
22. M. Kaplinghat, and A. Rajaraman, *Phys. Rev.* **D75**, 103504 (2007), astro-ph/0601517.
23. R. Bean, E. E. Flanagan, and M. Trodden, *Phys. Rev.* **D78**, 023009 (2008), 0709.1128.
24. C.-P. Ma, and E. Bertschinger, *Astrophys. J.* **455**, 7–25 (1995), astro-ph/9506072.
25. S. Hannestad, *Phys. Rev. Lett.* **95**, 221301 (2005), astro-ph/0505551.
26. G. La Vacca, S. A. Bonometto, and L. P. L. Colombo, *New Astron.* **14**, 435–442 (2009), 0810.0127.
27. B. A. Reid, L. Verde, R. Jimenez, and O. Mena (2009), 0910.0008.
28. J. Valiviita, R. Maartens, and E. Majerotto (2009), 0907.4987.